
Figures and figure supplements

Release-dependent feedback inhibition by a presynaptically localized ligand-gated anion channel

Seika Takayanagi-Kiya *et al*

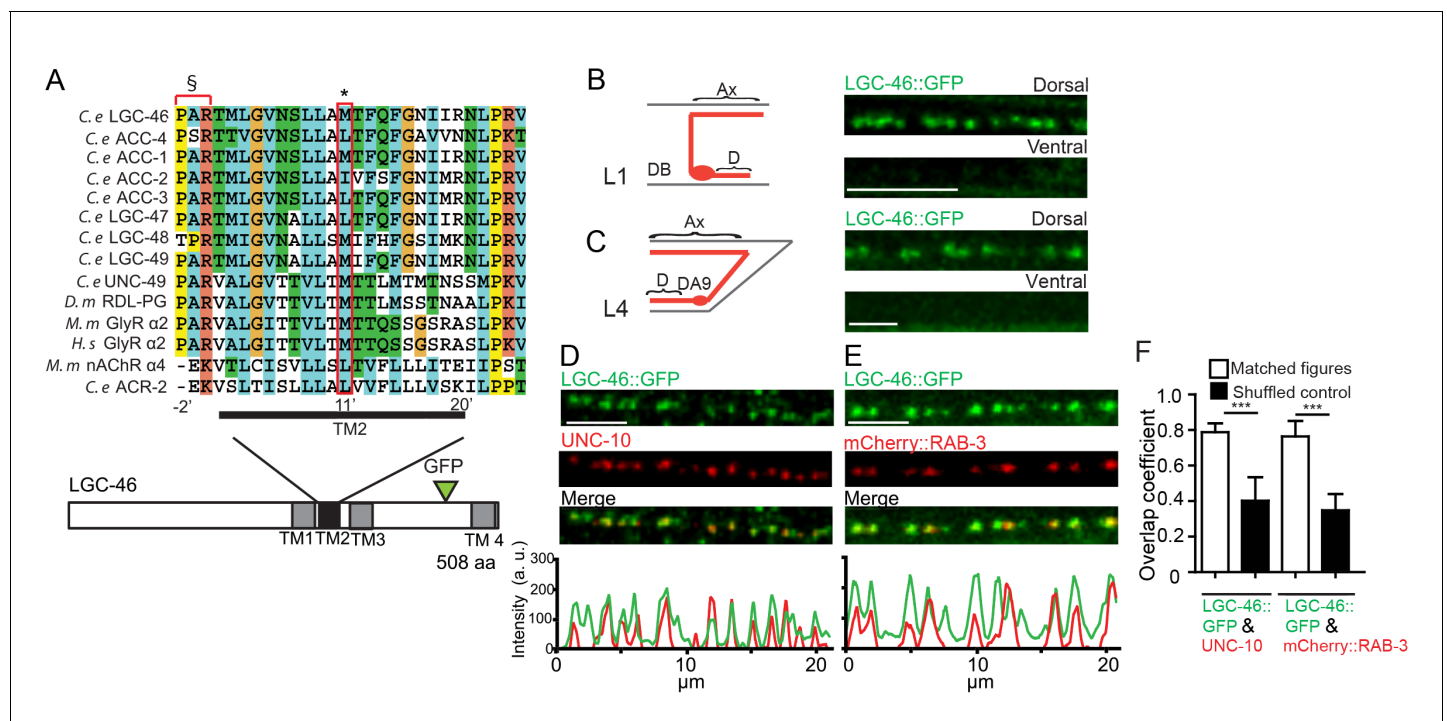


Figure 1. LGIC LGC-46 localizes to presynaptic terminals. (A) Alignment of TM2 of LGC-46 with other anion channels. * marks Met314, which is mutated to Ile in LGC-46(ju825). § marks PAR motif, a signature of ionotropic anion channels. (B–F) LGC-46::GFP localizes to presynaptic terminals of cholinergic motor neurons. (B) Left panel shows a schematic of a cholinergic motor neuron in L1 animals. Right panel shows a confocal image of LGC-46::GFP from *Punc-17β-LGC-46(WT)::GFP(juSi295)IV* showing punctate localization in the dorsal nerve cord. (C) Left panel shows a schematic of DA9 cholinergic motor neuron in the tail of L4 animals. Right panel shows LGC-46::GFP expressed in DA9 neuron, from *Pitr-1-LGC-46(WT)::GFP(juEx6843)*, showing punctate localization in the dorsal axon. (B, C): Ax: Axon. D: Dendrite. (D, E) LGC-46::GFP colocalizes with active zone protein UNC-10/RIM and synaptic vesicles in cholinergic motor neurons. Images of dorsal nerve cord are shown above, linescan analyses of fluorescent signal intensities below. (D) Confocal images of anti-GFP for LGC-46 (green) and anti-UNC-10 (red) from an animal carrying *Punc-17β-LGC-46(WT)::GFP(juSi295)IV*. (E) Presynaptic protein mCherry::RAB-3 expressed in cholinergic motor neurons overlapped with LGC-46::GFP signals. Images are from *Punc-17β-LGC-46(WT)::GFP(juSi295)IV; Pacr-2-mCherry::RAB-3(juEx7053)*. Scale bar: 5 μm. (F) Mander's overlap coefficient showing the extent of pixel colocalization of LGC-46 and presynaptic marker protein signals (open bar). As negative controls, Mander's overlap coefficient from shuffled images are shown (filled bar). n = 10 per genotype. Data shown as mean ± SD. Statistics: one way ANOVA followed by Tukey's post-hoc test. ***p < 0.001.

DOI: [10.7554/eLife.21734.002](https://doi.org/10.7554/eLife.21734.002)

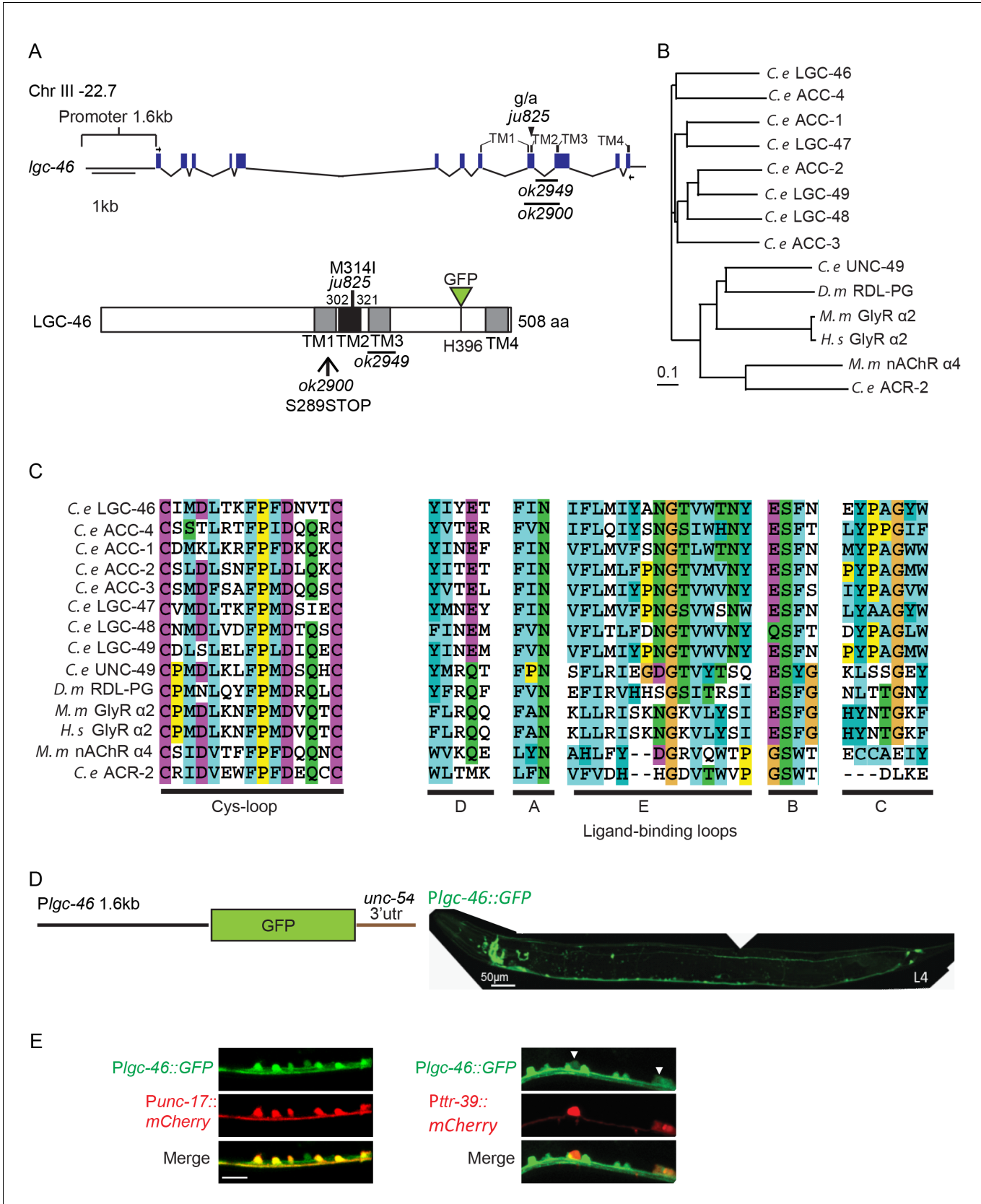


Figure 1—figure supplement 1. *lgc-46* is expressed in the nervous system including cholinergic motor neurons. (A) Gene and protein structure of *lgc-46*. The positions of the deletion alleles and the M314I mutation described in the text are noted. *ok2900* removes TM2 and TM3 and generates a

Figure 1—figure supplement 1 continued on next page

Figure 1—figure supplement 1 continued

premature stop codon, and *ok2949* generates an in-frame deletion which removes TM3. Arrows indicate the position of the primers used to amplify cDNA. Four transmembrane domains and the sites of mutations are noted in protein structure as well. For protein localization analysis, GFP was inserted at the cytoplasmic loop between TM3 and TM4. (B) Phylogenetic tree of LGICs shows that LGC-46 is a member of the ACC family of proteins from *C. elegans* (ACC-1 to ACC-4, LGC-46 to LGC-49). Generated by ClustalX2 using the neighbor-joining method (Larkin et al., 2007). (C) Amino acid sequence alignment of the Cys-loop region, and regions corresponding to the ligand-binding loops of nAChR. (D) (Left) Illustration of *Plgc-46* transcriptional reporter. (Right) *Plgc-46*-GFP expression in a L4 animal is seen in the nervous system including the ventral nerve cord. (E) Expression of *Plgc-46*-GFP overlaps with cholinergic motor neuron-specific (*Punc-17-mCherry*) and GABAergic motor neuron-specific (*Pttr-39-mCherry*) markers.

DOI: [10.7554/eLife.21734.003](https://doi.org/10.7554/eLife.21734.003)

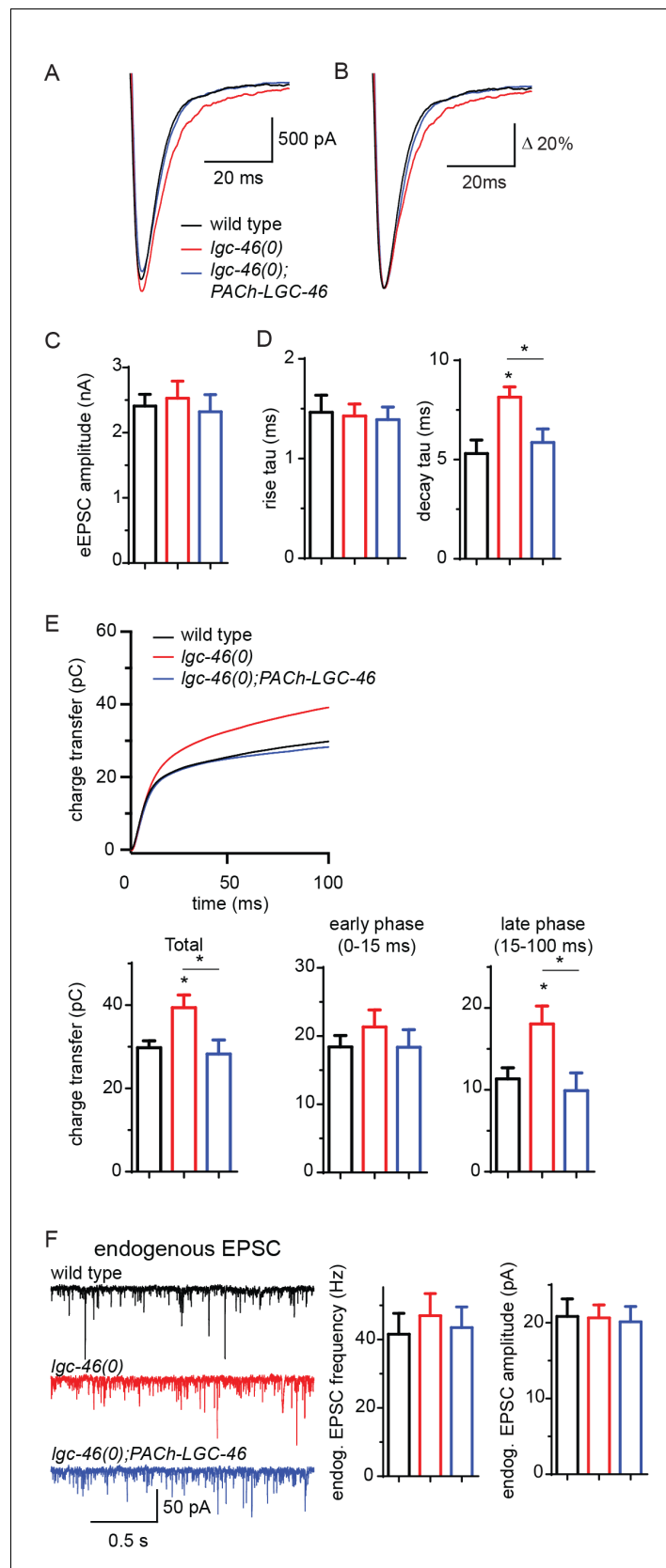


Figure 2. LGC-46 regulates the decay phase of eEPSCs to modulate the late phase of SV release. (A and B) Average traces (A) and normalized average traces (B) of eEPSCs. (C) Mean amplitude of eEPSCs. (D) Rise tau and decay tau of eEPSCs. (E) Charge transfer of eEPSCs. (F) endogenous EPSC. Figure 2 continued on next page

Figure 2 continued

decay tau of eEPSCs. (E) Average traces of cumulative charges of eEPSCs, and charge transfers after stimulation. (F) Representative traces, mean frequency and mean amplitude of endogenous EPSCs. wild type ($n = 11$), *lgc-46(ok2900)* ($n = 10$), and *lgc-46(ok2900); PACH-LGC-46* ($n = 11$). Animals were recorded at 20 degrees in 1.2 mM Ca^{2+} bath solutions. Statistics, one-way ANOVA, Bonferroni's post hoc test. * $p < 0.05$. Error bars indicate SEM.

DOI: [10.7554/eLife.21734.004](https://doi.org/10.7554/eLife.21734.004)

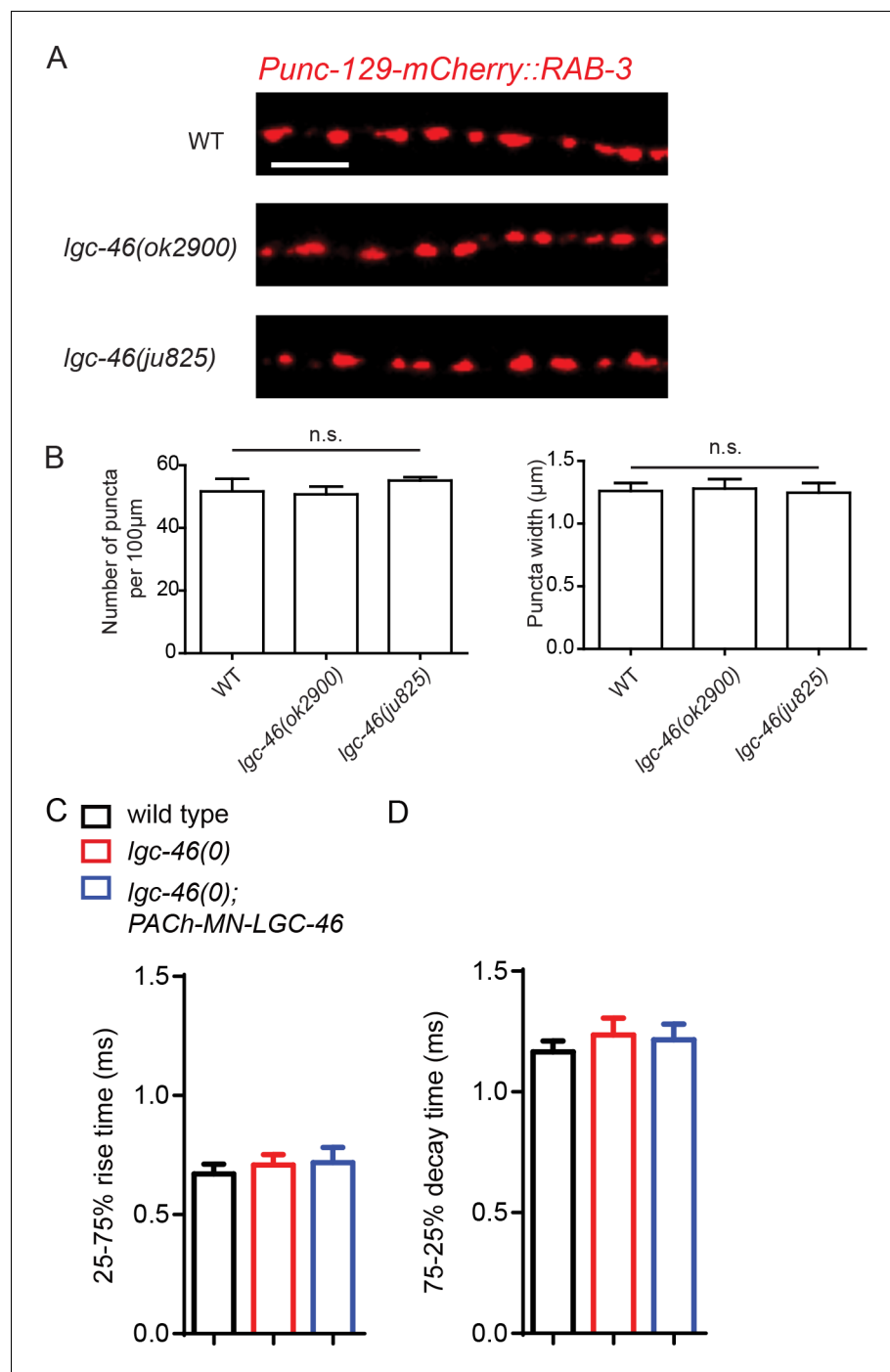


Figure 2—figure supplement 1. Morphology of cholinergic synapses as well as the amplitude and kinetics of endogenous EPSCs are normal in *lgc-46(0)*. (A) Representative images of mCherry::RAB-3 puncta in the dorsal nerve cord from each genotype. Scale bar: 5 μm . (B) Quantification of the puncta density and width show no significant differences between the wild type, *lgc-46(ok2900)* and *lgc-46(ju825gf)* backgrounds. Data shown as mean \pm SEM, $n = 6$ animals (20 μm per animal) per genotype. Scale bar: 5 μm . (CD) 25%–75% rise time (C) and 75%–25% decay time (D) of endogenous EPSCs. $n = 10$ to 12 for all animals. Statistics, one way ANOVA and Bonferroni's post hoc test. Error bars indicate SEM.

DOI: [10.7554/eLife.21734.005](https://doi.org/10.7554/eLife.21734.005)

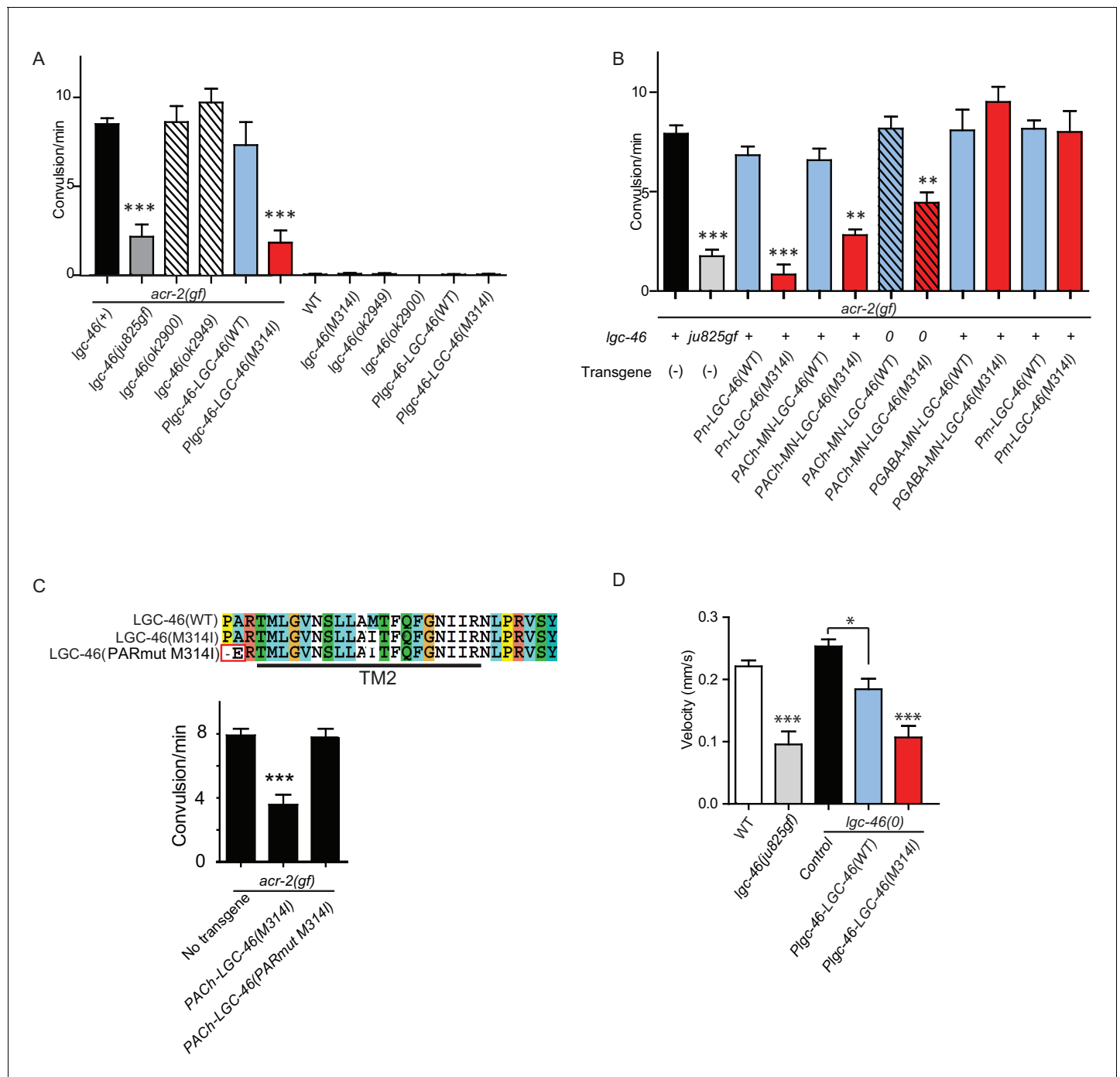


Figure 3. A gain-of-function mutation LGC-46(M314I) affects excitation and inhibition imbalance in locomotor circuit. (A) Quantification of convulsion frequencies. *lgc-46(ju825)*, but not *lgc-46(0)*, suppresses *acr-2(gf)* convulsions. Overexpression of LGC-46(M314I) under its own promoter also strongly suppresses convulsion. Data shown as mean \pm SEM; $n \geq 16$. (B) Overexpression of LGC-46(M314I) in cholinergic motor neurons can suppress *acr-2(gf)* convulsions. Data shown as mean \pm SEM; $n \geq 16$. Promoters used to drive expression are, *Prgef-1* for neurons, *Punc-17b* for cholinergic motor neurons, *Punc-25* for GABAergic motor neurons, *Pmyo-3* for muscles (See [Supplementary file 1,2](#)). (A and B) Statistics: one-way ANOVA followed by Dunnett's post-hoc test. ** $p < 0.01$, *** $p < 0.001$. (C) (Top) Amino acid sequences of LGC-46 wild type, M314I, and PAR motif mutant M314I. (Bottom) Convulsion frequencies of each genotype are shown. Cholinergic motor neuron-specific expression of LGC-46(M314I) suppresses *acr-2(gf)* convulsions, whereas the PAR motif mutant LGC-46(P301A A302E M314I) does not. Data shown as mean \pm SEM; $n = 24, 16, 16$, respectively. Statistics: one way ANOVA followed by Dunnett's post-hoc test. * $p < 0.05$, *** $p < 0.001$. (D) Off-food velocities for each genotype. Statistics: one-way ANOVA followed by Bonferroni's post-hoc test. Data shown as mean \pm SEM. ** $p < 0.01$, *** $p < 0.001$.

DOI: [10.7554/eLife.21734.006](https://doi.org/10.7554/eLife.21734.006)

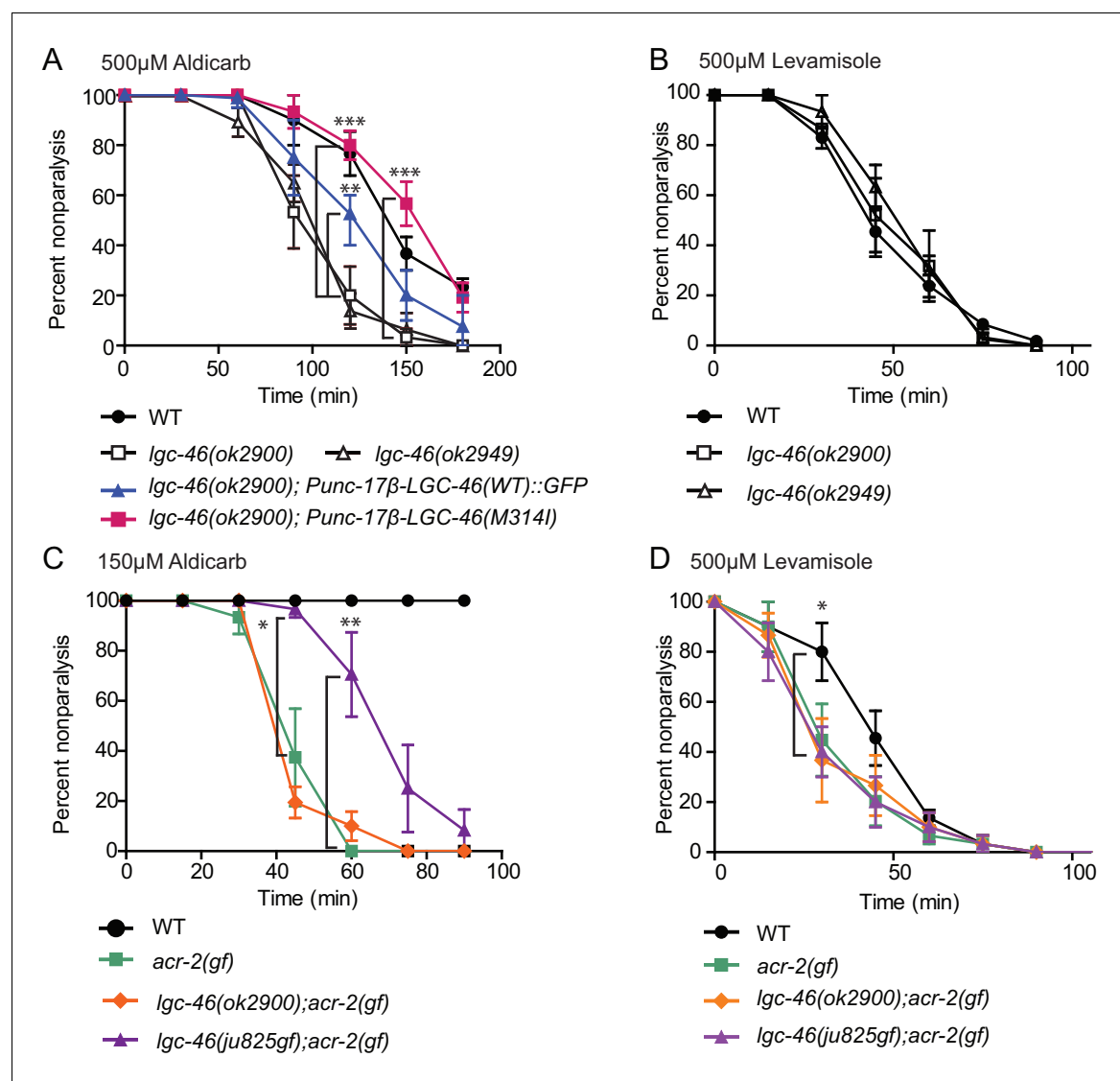


Figure 3—figure supplement 1. Pharmacological assays of aldicarb and levamisole. (A) *lgc-46(ok2900)* is hypersensitive to aldicarb hypersensitivity, which is suppressed by cholinergic motor neuron-specific expression of functional LGC-46::GFP. (B) *lgc-46(0)* alleles do not affect levamisole sensitivity. (C,D) *lgc-46(M314I)* partially suppresses the aldicarb hypersensitivity (C) but not levamisole hypersensitivity (D) of *acr-2(gf)*. Results are from three independent trials. $n = 15$ for one group per trial. Mean rate of paralysis at each time point are shown. Error bars indicate SEM. Statistics: **: $p < 0.01$, *: $p < 0.05$ by two-way ANOVA and Bonferroni post-hoc test.

DOI: [10.7554/eLife.21734.007](https://doi.org/10.7554/eLife.21734.007)

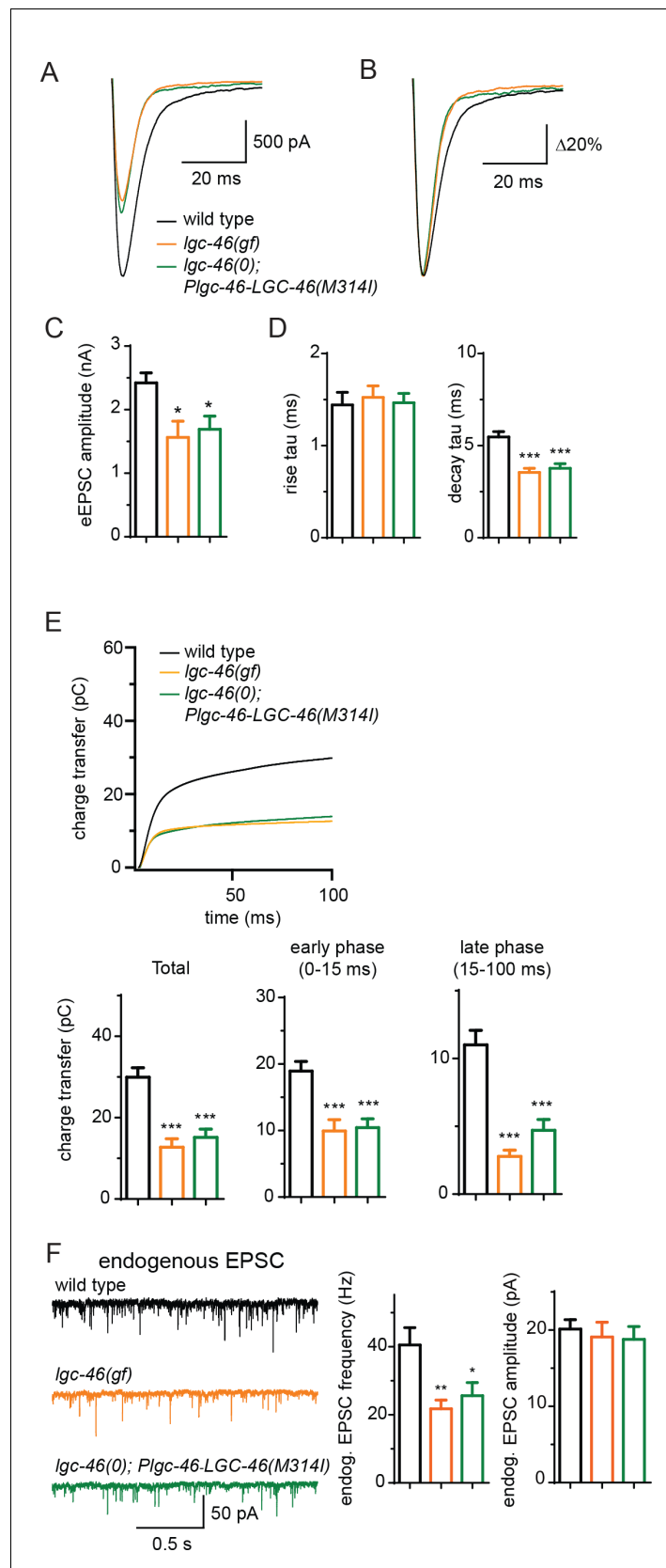


Figure 4. LGC-46(M314I) limits synaptic transmission by shortening the decay phase of evoked release. (**A** and **B**) Average traces (**A**) and normalized average traces (**B**) of eEPSCs. (**C**) Mean amplitude of eEPSCs. (**D**) Rise tau and decay tau of eEPSCs. (**E**) Charge transfer of eEPSCs. (**F**) endogenous EPSC. * indicates $p < 0.05$, ** indicates $p < 0.01$, *** indicates $p < 0.001$. Figure 4 continued on next page

Figure 4 continued

decay tau of eEPSCs. (E) Average traces of cumulative charges of eEPSCs, and charge transfers after stimulation. (F) Representative traces, mean frequency and mean amplitude of endogenous EPSCs. wild type (n = 12), *lgc-46(ju825gf)* (n = 10), and *lgc-46(0);Plgc-46-LGC-46(M314I)* (n = 12). Animals were recorded at 20 degrees in 1.2 mM Ca^{2+} bath solutions. Statistics, one-way ANOVA, Bonferroni's post hoc test. ***p<0.001, **p<0.01, *p<0.05. Error bars indicate SEM.

DOI: [10.7554/eLife.21734.008](https://doi.org/10.7554/eLife.21734.008)

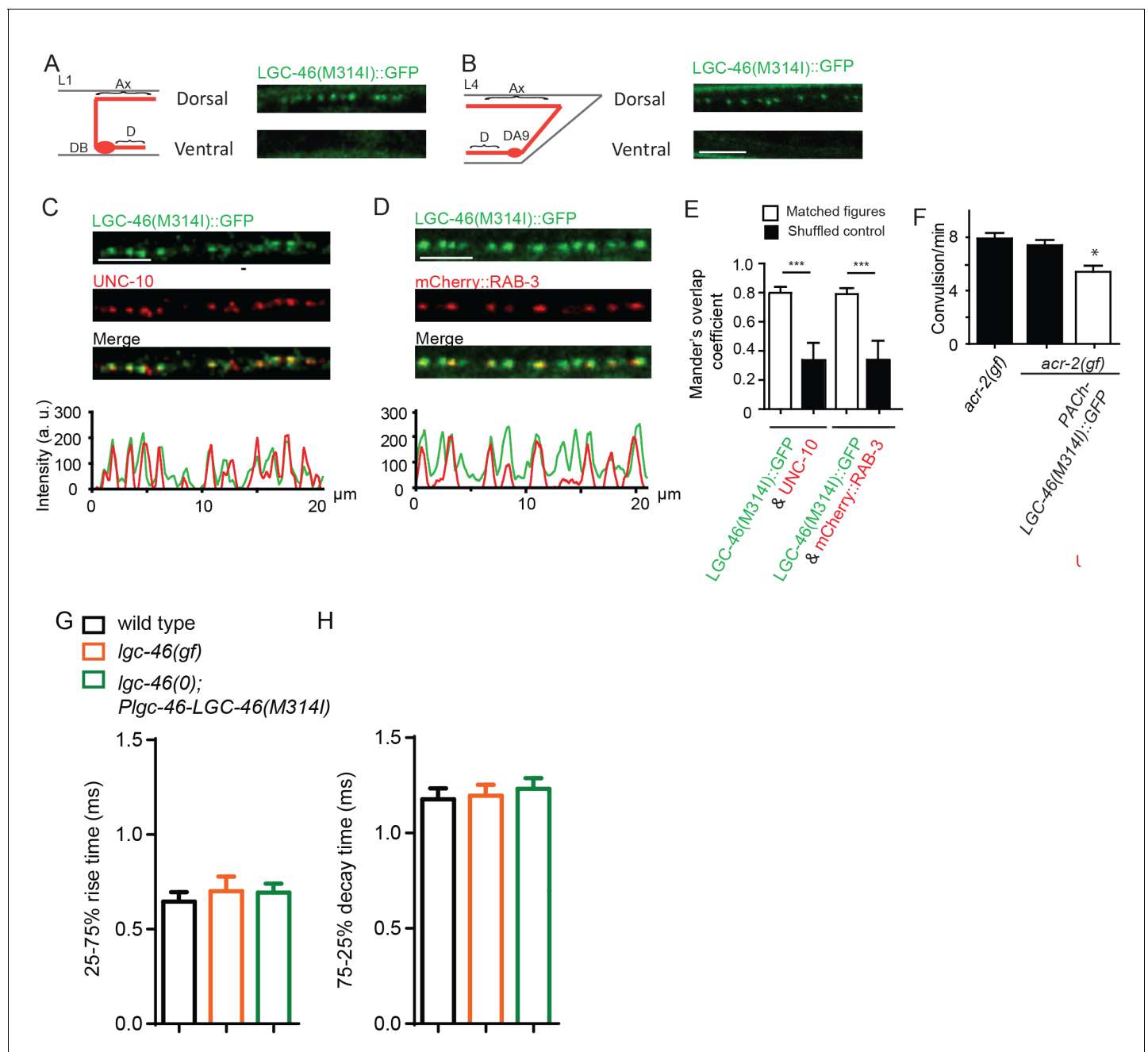


Figure 4—figure supplement 1. LGC-46(M314I) shows a presynaptic punctate localization pattern similar to LGC-46(WT), and amplitude and kinetics of endogenous EPSCs are normal in *lgc-46(gf)*. **(A–D)** Confocal images of animals expressing LGC-46(M314I)::GFP in cholinergic motor neurons. **(A)** (Left panel) Schematic of a cholinergic motor neuron in L1 animals. (Right panel) LGC-46(M314I)::GFP shows punctate localization on the dorsal process of cholinergic motor neurons of L1 animals. Images are from *Punc-17β-LGC-46(M314I)(juSi282)IV*. **(B)** (Left panel) Schematic of a cholinergic motor neuron DA9 in L4 animals. (Right panel) LGC-46(M314I)::GFP expressed in DA9 neuron shows punctate signals in the dorsal process in L4 animals, indicating their axonal localization. Images are from *Pitr-1-LGC-46(M314I)::GFP(juEx6845)*. **(C,D)** Presynaptic proteins colocalize with LGC-46(M314I)::GFP in cholinergic motor neurons. Images taken from the dorsal nerve cord are shown. Lower panels show the linescan of fluorescent signal intensities. **(C)** Anti-GFP and anti-UNC-10 signals from an animal carrying *Punc-17β-LGC-46(M314I)(juSi282)IV*. **(D)** Presynaptic protein mCherry::RAB-3 expressed in cholinergic motor neurons overlapped with LGC-46(M314I)::GFP signals. Images are from *Punc-17β-LGC-46(M314I)(juSi282)IV; Pacr-2-mCherry::RAB-3(juEx7053)*. **(E)** Mander's overlap coefficient showing the extent of pixel colocalization of LGC-46 and pre synaptic marker protein signals (open bar). As negative controls, Mander's overlap coefficient from shuffled images are shown (Filled bar). For each genotype, 10 images were analyzed. Data shown as mean ± SD. Statistics: one way ANOVA followed by Tukey's post-hoc test. ***: $p < 0.001$. **(F)** Single copy insertion allele *Punc-17β-LGC-46(M314I)(juSi282)IV* can significantly suppress the *acr-2(gf)* convulsion frequency. Data shown as mean ± SEM; $n = 20, 16, 16$, respectively. **(G–H)** 25%–75% rise and decay times of endogenous EPSCs are normal in *lgc-46(gf)*. Figure 4—figure supplement 1 continued on next page

Figure 4—figure supplement 1 continued

time (G) and 75%–25% decay time (H) of endogenous EPSCs. $n = 10$ to 12 for all animals. Statistics, one way ANOVA and Bonferroni's post hoc test. Error bars indicate SEM.

DOI: [10.7554/eLife.21734.009](https://doi.org/10.7554/eLife.21734.009)

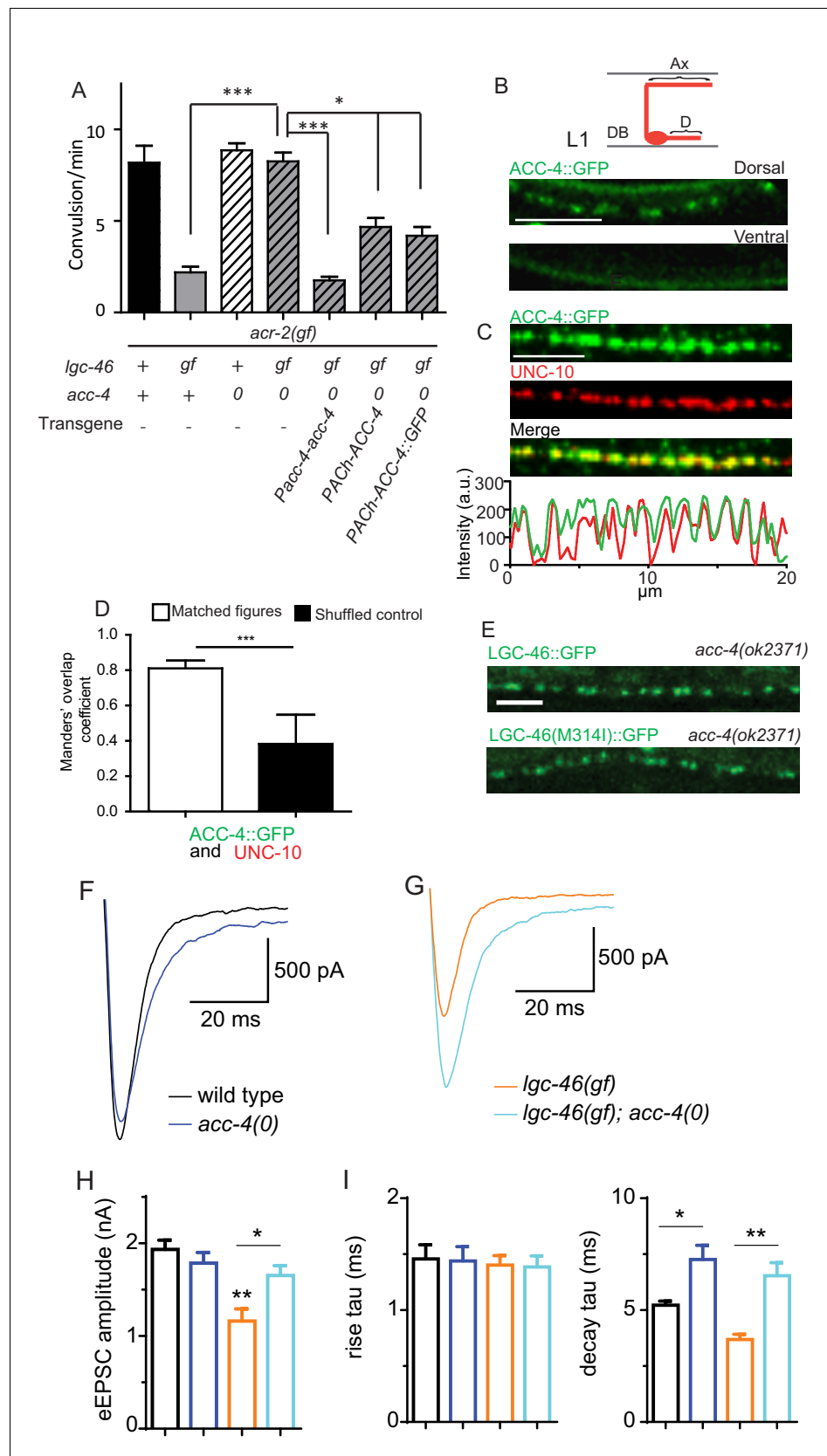


Figure 5. ACC-4 is required for the function of LGC-46(M314I), and localizes presynaptically. (A) Frequency of convulsion in animals of indicated genotypes. Loss of function in *acc-4* reverses the suppression effect by *lgc-46*
 Figure 5 continued on next page

Figure 5 continued

(*ju825*) on *acr-2(gf)*. The expression of *acc-4(+)* under the endogenous promoter or cholinergic motor neuron-specific promoter can rescue the effect. Data shown as mean \pm SEM; $n \geq 16$. Statistics: one way ANOVA followed by Dunnet's post-hoc test. $**p < 0.01$, $***p < 0.001$. (BD) ACC-4::GFP localizes to presynaptic terminals of cholinergic motor neurons, similar to LGC-46::GFP. Images are from *lgc-46(gf) acc-4(0)*; *acr-2(gf)*; *Punc-17b-acc-4::GFP* (*juEx7438*). (B) Upper panel shows a schematic of a cholinergic motor neuron in L1 animals. The lower panel shows a confocal image of ACC-4::GFP showing punctate localization in the dorsal nerve cord. (C) ACC-4::GFP colocalizes with active zone protein UNC-10/RIM. (D) Mander's overlap coefficient showing the extent of pixel colocalization of ACC-4 and UNC-10 (open bar) from immunostaining. As negative controls, Mander's overlap coefficient from shuffled images are shown (Filled bar). For each genotype, 10 images were analyzed. Data shown as mean \pm SD. Statistics: Student's t-test. $***p < 0.001$. (E) The punctate localization of LGC-46 is maintained in the *acc-4(ok2371)* null mutants. (F and G) Average traces of evoked release (eEPSC) from wild type ($n = 10$), *acc-4(0)* ($n = 10$), *lgc-46(gf)* ($n = 10$), and *lgc-46(gf);acc-4(0)* ($n = 10$). (H) Mean amplitude of eEPSC. (I) Rise tau and decay tau of eEPSC. Animals were recorded at 17°C in 2 mM Ca^{+} bath solutions. Statistics, one-way ANOVA. Bonferroni's post hoc test for eEPSC comparisons. $**p < 0.01$; $*p < 0.05$. Error bars indicate SEM.

DOI: [10.7554/eLife.21734.010](https://doi.org/10.7554/eLife.21734.010)

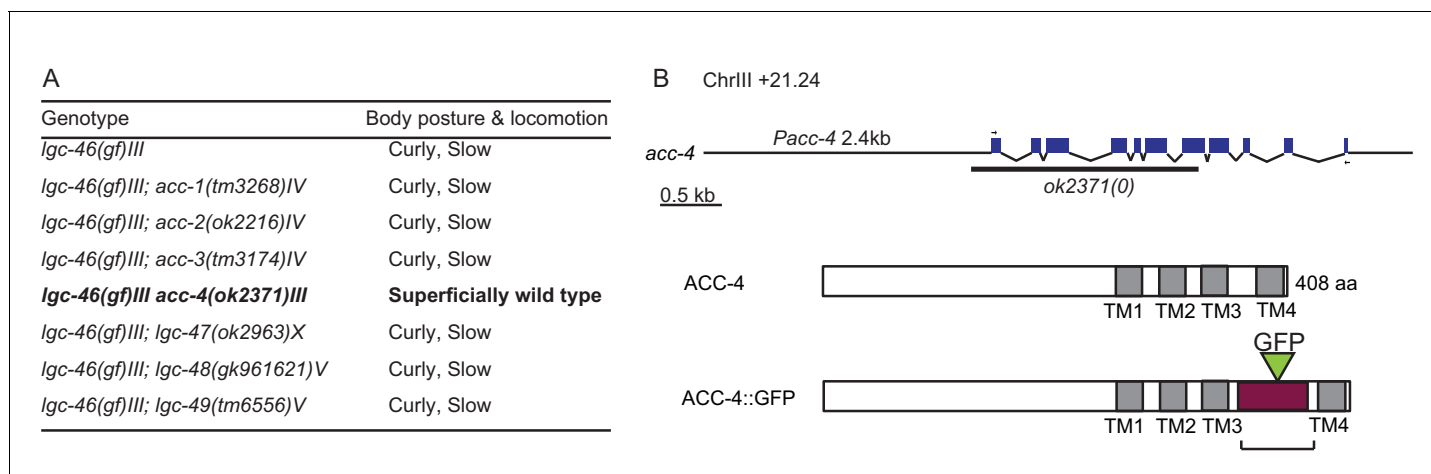


Figure 5—figure supplement 1. ACC-4 is required for the function of LGC-46(M314I). (A) Locomotion observed in double mutants of *lgc-46(ju825gf)* and *acc* group genes. (B) Gene and protein structure of *acc-4*. Arrows indicate the position of the primers used to amplify cDNA. In ACC-4::GFP, the box filled with purple indicates the region where the GFP-tagged intracellular loop of LGC-46 was inserted.

DOI: 10.7554/eLife.21734.011